Applying Silver Tellurite to Optimize Ag/Si Contact Interface in Silicon Solar Cells①

LIU Jian ZHAO Qing-He YANG Lu-Yi
LIN Yuan PAN Feng②
(*School of Advanced Materials, Peking University, Shenzhen Graduate School, Shenzhen* 518055, *China*)

ABSTRACT Nowadays, researches on developing new etching materials to optimize the Ag/Si contact interface in silicon solar cells (SSCs) are rare, which alleviates the further development of SSCs. In this study, silver tellurite (Ag_2TeO_3, monoclinic, $P2_1/a$(14)) is synthesized and developed as an excellent etching material in SSCs. The Ag_2TeO_3 displays a low starting temperature of etching Si_3N_4 of ~545 °C, which is ~160 °C lower than that of PbO. Besides, by applying Ag_2TeO_3, conductive silver nanoparticles with a length of about 300~500 nm and a thickness of ~50 nm form in the Ag/Si contact interface, which effectively reduces the Ag-Si contact resistance, and leads to a high solar cell efficiency of ~18.4%. This study opens a new window for further enhancing the solar cell efficiency in the future.

Keywords: silver tellurite, solar cell, silicon nitride, Ag-Si contact, solar cell efficiency;
DOI: 10.14102/j.cnki.0254–5861.2011–2779

1 INTRODUCTION

Photovoltaic power generation is one of the most promising sources of renewable clean energies, in which the SSCs account for more than ~90% of the photovoltaic market share. Developing high-efficiency SSCs is the future direction, and one of the key issues to improve the solar cell efficiency is optimizing Ag/Si contact interface during metallization process[1, 2]. Screen printing of silver paste and high-temperature sintering have been applied to achieve the metallization in the large-scale production of SSCs. Thus, the sintering mechanism[3] and Ag/Si ohmic contact mechanism are research hotspots in the research field of SSCs. Some factors affecting electrochemical properties of the Ag-Si ohmic contact are listed as follows: sintering process[3, 4], interface morphology of Ag/Si contact interface[5-15], glass composition of siver paste[16-24] and cell structure [25](Fig. 1). Chung et al.[3] have investigated the influence of O_2 on Ag ionization in molten lead borosilicate glass during sintering process, in which the Ag powder can dissolve into the molten glass as Ag^+ ions via the interaction of silver with oxygen in ambient atmosphere, the increased P_{O2} can increase the Ag^+concentration in the molten glass, and plays a crucial role on the fire-through Ag/Si contact formation. Dieter K et al. have reviewed the ohmic contact of SSCs[4], in which some basic principles for Ag-Si contanct are demonstrated, including the tunnelling mechanism, Fermi level pinning, field emission, thermal/field

Received 13 February 2020; accepted 19 February 2020
① This work was financially supported by Soft Science Research Project of Guangdong Province (No. 2017B030301013), Guangdong Innovative Team Program (No. 2013N080), and Shenzhen Science and Technology Research Grant (No. JSGG20170414163208757)
② Corresponding author. E-mail: panfeng@pkusz.edu.cn
The firs two authors contriute equally to this work

emission, as well as current transport of surface states. The Ag-Si contact formation process has also been reported, as well as the optimization of formulation and sintering process to achieve high-performance solar cell silver paste[5, 6]. Cheng et al. have investigated the two-dimension distribution of Ag crystallites for SSCs sintering at different temperature, in which their microstructural observations give new insights into the tunneling mechanism of current flow of Ag/Si interface from under-fired to over-fired conditions[8].

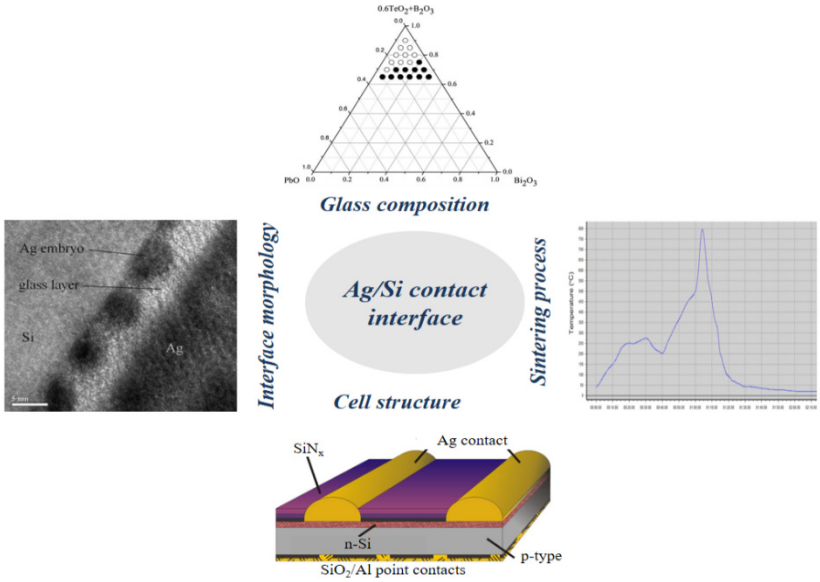

Fig. 1. Factors affecting Ag/Si contact interface: sintering process[18], copy right of Elesver; interface morphology[7], copy right of Elesver; glass composition[16], copy right of Elsever; and cell structure[25], copyright of IEEE

The interface morphology of Ag/Si contact interface has also been intensely reported. Usually, the nano-structure of Ag/Si interface contains a mixture of contact features such as ultra-thin interface glass, nano-scale Ag precipitating in the ultra-thin interface glass, and sub-micron Ag crystallites at the Si surface[9, 10]. It is reported that a uniform ultra-thin interfacial glass containing nano-Ag colloids can be formed in the Ag/Si contact interface under opitimally-fired conditions with enhanced solar cell performance due to the reduced contact resistivity[8]. Under over-fired condition, some Ag crystallites attach into the Si emitter surface and significantly disturb the potential distribution, resulting in lowered solar cell performance. Thus, the size of large Ag crystallites at Si emitter surface shall be kept to a minimum[12].

The interface morphology of Ag/Si contact is vital for improving the photoelectric conversion efficiency of the SSCs. By tuning the glass composition, the Ag/Si contact interface can be optimized. For a typical silver paste, it usually consists of three constituents: silver particles as the conductive phase, glass frit as inorganic binder, and organic compounds as dispersant. Despite the minor content (< 8 wt%) in silver paste, the glass frit plays a key role on forming fine contact between the silver and silicon wafer[10, 11]. Some basic functions of glass frit include etching the reflective layer Si_3N_4, forming a Ag-Si ohmic contact with the silicon substrate, and so on. During sintering process, the glass melts can wet and dissolve the Ag powder at the sintering temperature by generating a liquid glassy-phase. Besides, this glassy-phase can flow downward to the surface of SSCs to etch through the SiNx anti-reflection layer (70~80 nm)[4]. Various kinds of glass frits have been developed, such as TeO_2-based[17], Pb-Te-O based[18-22], abd Lead-free glass frits[23] and so on. For example, a

new type of lead-free silver paste using a TeO_2-based glass as the front electrode of SSCs has been reported by Cai et al., which shows a resistance of about 3.1~3.7 μΩ cm after sintering[17]. Pi et al. have studied the effects of glass powder on the etching process of the Si_3N_4 antireflection film and silver resistivity, and reveal that tellurium glass can make the combination of silver and silicon better[21].

Finding and developing new etching materials for the metallization of SSCs, realizing low-temperature sintering, lead-free[23] and studying the related function performance and mechanism are an important topic for solar cell metallization. As a rarely reported compound, the research on properties of Ag_2TeO_3 as etching material in SSCs is rather lacking. The synthetic method of Ag_2TeO_3 has been reported by Sharma et al.[25]. In this study, the Ag_2TeO_3-based glass frit is applied to further optimize the Ag/Si contact interface of SSCs. Besides, the corresponding optimization mechanism is also demonstrated.

2 OPTIMIZATION MECHANISM OF Ag_2TeO_3-BASED GLASS FRIT

Ag_2TeO_3 was directly synthesized by $AgNO_3$ (purity 99.9%) with TeO_2 (purity 99.99%, particle size D50 = 100 nm). The mixture is evenly mixed and annealed in a muffle furnace at 750 °C for 100 min. Then the obtained Ag_2TeO_3 is ball-milled to powder with an average particle size D_{50} = 10 μm. X-ray diffraction (XRD, Bruker, D8) is applied to characterize the phase structure of the synthesized Ag_2TeO_3 (Fig. 2a), which is consistent with the PDF card of #83-1779, indicating the successful synthesis of Ag_2TeO_3. The Ag_2TeO_3 phase belongs to a $P2_1/a$(14) space group with monoclinic phase structure. Compared with the previous report[24], the synthesis of Ag_2TeO_3 in this study is much simple, and the direct solid-reaction of $AgNO_3$ and TeO_2 can also avoid the contamination of other metal ions and improve the experimental quality.

The TGA and DSC curves of the mixture of Ag_2TeO_3 with Si_3N_4 (Fig. 2b) indicates that the redox reaction between Ag_2TeO_3 with Si_3N_4 starts at ~545 °C, which is much lower than the melting temperature of Ag_2TeO_3 with Si_3N_4, indicating a solid reaction. Besides, from the DSC curves, we also reveal that the redox exothermic reaction mainly occurs around ~600 °C, which is beneficial to increase the temperature of the system and accelerate the reaction. During the redox reaction process, N_2 is released, and the corresponding reactions are shown as equations (1) and (2):

$$6Ag_2TeO_3 + Si_3N_4 = 12Ag + 3SiO_2 + 6TeO_2 + 2N_2\uparrow \quad (1)$$

We also observe that the TGA curve begins to increase at ~750 °C, and it reaches the highest point at ~900 °C, indicating that the reaction in this period is dominated by equation 2. Meanwhile, beyond ~800 °C, the weight gains in TGA curve are obvious, while exothermic heat is weak, which may demonstrate that the endothermic reaction of the system absorbing oxygen and the exothermic reaction of the etching reaction may cancel out each other, so there is no obvious dynamic change of energy.

$$2Ag_2TeO_3 + Si_3N_4 + 2O_2 = 4Ag + 3SiO_2 + 2TeO_2 + 2N_2\uparrow \quad (2)$$

Fig. 2c depicts the comparison of TGA curve of Ag_2TeO_3 and PbO with Si_3N_4, respectively, which shows a significant difference. For PbO reacting with Si_3N_4, the mass remains stable until ~700 °C. Above this temperature, an obvious weight gain is observed, which is very different from that of Ag_2TeO_3 reacting with Si_3N_4. This result indicates that the O_2 in atmosphere mainly dominates the etching reaction for PbO. The corresponding reaction is as equations (3) and (4).

$$6PbO + Si_3N_4 = 6Pb + 3SiO_2 + 2N_2 \quad (3)$$

$$2Pb + O_2 = 2PbO \quad (4)$$

Besides, the etching reaction of Ag_2TeO_3 and Si_3N_4 starts at about ~540 °C, which is ~160 °C lower than that of the traditional PbO. Thus, the advantage of Ag_2TeO_3 lies in the lower reaction

temperature and more abundant oxygen source.

TEM together with EDS is also applied to analyze Ag/Si contact interface after introducing Ag_2TeO_3-based glass frit. Fig. 2d indicates that the silver particle generates along the surface of silicon, with length of about 300~500 nm and thickness of 50 nm, which is the product of etching reaction of Ag_2TeO_3 and Si_3N_4 in the glass. The micro-region of the silver-silicon contact is also presented, in which the charges can transport or tunnelling from the silicon emitter surface to the silver grid to achieve the collection and transport of charges[8]. Fig. 2e shows the EDS-mapping results of the silicon-silver contact micro-region. It can be seen that the Ag and O in the silicon-silver contact interface is distributed separately, so the interface etching product is pure silver particles.

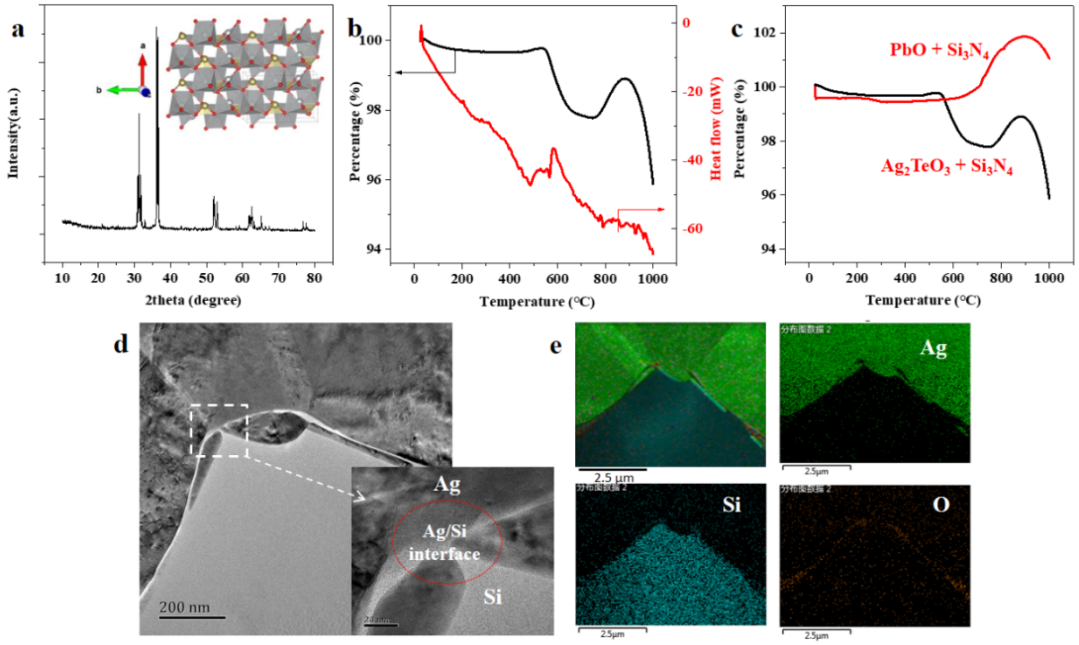

Fig. 2. Optimizing Ag/Si contact interface with Ag_2TeO_3-based glass frit. (a) X-ray diffraction pattern of Ag_2TeO_3, and corresponding crystal structure (inset, grey sphere represents the Ag atom, yellow sphere the Te atoms, and red spheres the O atom); (b) DSC/TGA curves of Ag_2TeO_3 reacting with Si_3N_4 in oxygen-containing atmosphere; (c) Thermos-gravimetric curves of Ag_2TeO_3 and PbO reacting with Si_3N_4 in O_2 atmosphere, respectively; (d) TEM morphologies of the cross-section Ag/Si contact interface, and (e) Corresponding EDS-mapping images

To confirm the optimizing performance of Ag_2TeO_3 based glass frit, the solar cells are assembled and tested. The maximum current density of the solar cell reaches 38.37 mA/cm^2, the open voltage is about 0.638 V, and the photoelectric conversion efficiency is up to 18.41%, with an average value larger than ~18%, proving that the silver grid of solar cells using Ag_2TeO_3 as etching material presents good charge collection ability.

The distribution position and morphology of silver particles have a great influence on the solar cell performance. L. Liang et al. have studied the key features on the interface micro-regions of the solar cell. In addition to some residual SiN_x, the major components are a thin glass layer with nano-Ag colloids, and the size of Ag particles on the surface of the silicon emitter is about 10~100 nm[10]. It can also be seen apparently that the silver particles distribute discretely on the interface with the average distances more than ~50 nm, which is disadvantage for the charge collection. C. Ballif et al. have studied the resistance of the direct contact between silver and silicon, and find that the resistivity in some regions was four orders of magnitude lower than the typical

value[5], indicating that the contact between silver and silicon could significantly reduce the contact resistance of the solar cell and collect the charge better. Besides, C. Ballif et al. have also revealed that the silver-silicon contact interface is composed of Ag crystals with size of about 200~500 nm, and with an average penetration of ~130 nm into silicon. They consider that the silver is grown from glass melts, and similarly, the silver particles also exhibit discrete distribution[13], which is also harmful for the charge collection. In this study, the silver nanoparticles are shown as strips in the silicon-silver contact interface, indicating that a higher concentration of silver ions is provided in the process of growth due to the addition of Ag_2TeO_3 in the glass (Fig. 3), that's to say, Ag_2TeO_3 can produce more silver in the silicon-silver contact interface after etching Si_3N_4, thus enabling the continuous distribution of silver particles, which can directly contact with silicon to collect charge, and output through a silver grid and then improve the solar cell efficiency.

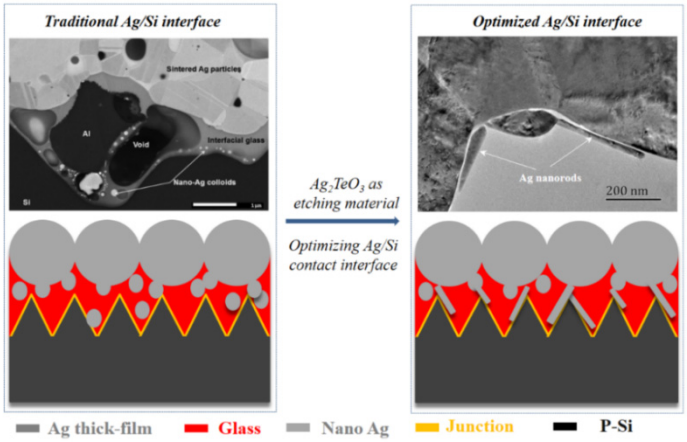

Fig. 3. Optimization mechanism of Ag_2TeO_3-based glass frit on the Ag/Si contact of silicon solar cells

From the above results, it can be seen that the addition of Ag_2TeO_3 to the glass of silver paste, on the one hand, can realize the low temperature sintering of silver grid, and on the other hand, the product of the reaction between Ag_2TeO_3 and Si_3N_4 is conductive metal silver, which presents much higher conductivity advantage than other materials, and the effect of improving the efficiency of silicon solar cells is particularly prominent.

3 SUMMARY & PERSPECTIVE

In summary, in this study, the Ag_2TeO_3-based glass frit is applied to further optimize the Ag/Si contact interface of SSCs, and thus effectively improve the solar cell effeciency. The starting temperature of Ag_2TeO_3 etching Si_3N_4 is ~545 °C, which is about ~160 °C lower than that of the traditional PbO etching agent. By applying the Ag_2TeO_3-based glass frit, the solar cells obtain a high current density of ~38.37 mA/cm^2 for Ag_2TeO_3-containing solar cells, an open voltage about ~0.638 V, as well as an average efficiency of more than 18%. This outstanding solar cell performance is mainly due to the optimized Ag/Si contact interface. The silver-silicon interface was observed by TEM/EDS, which indicates that silver nanoparticles are observed continuously distributing on the silicon-silver contact interface, with a length of about 300~500 nm, and a thickness of ~50 nm. This kind of silver can collect and transmit charge better, and thus can reduce contact resistance and improve solar cell efficiency. This study opens up a new direction for the metallization of silicon solar cells from the perspective of material development, and also promotes the development of low-temperature sintered silver paste with less lead or lead-free.

REFERENCES

(1) Kumara, P.; Aabdinb, Z.; Pfeffera, M.; Eibla, O. High-efficiency, single-crystalline, p- and n-type Si solar cells: microstructure and chemical analysis of the glass layer. *Sol. Energy Mat. Sol. C* **2018**, 178, 52–64.

(2) Corsin, B.; Andres, C.; Stefaan, D. High-efficiency crystalline silicon solar cells: status and perspectives. *Energy Environ. Sci*. **2016**, 9, 1552–1576.

(3) Chung, B.; Cho, S.; Chun, J.; Kim, Y.; Okamoto, K.; Huh, J. Influence of oxygen on Ag ionization in molten lead borosilicate glass during screen-printed Ag contact formation for Si solar cells. *Electrochimica Acta* **2013**, 106, 333–341.

(4) Schroder, D.; Meier, D. Solar cell contact resistance-a review. *IEEE. Tran. EL*. **1984**, 5, 637–647.

(5) Ballif, C.; Huljić, G.; Willeke, H.; Wyser, A. Silver thick-film contacts on highly doped n-type silicon emitters: structural and electronic properties of the interface. *Appl. Phys. Lett*. **2003**, 82, 1878–1880.

(6) Xiong, S.; Li, Y.; Liu, C.; Yuan, X.; Tong, H.; Yang, Y.; Ye, X.; Wang, X.; Luo, L. Rapid and accurate characterization of silver-paste metallization on crystalline silicon solar cells by contact-end voltage measurement. *AIP Advances* **2018**, 8, 095225.

(7) Lin, C.; Tsai, S.; Hsu, S.; Hsieh, M. Investigation of Ag-bulk/glassy-phase/Si heterostructures of printed Ag contacts on crystalline Si solar cells. *Sol. Energy Mat. Sol. C* **2008**, 92, 1011–1015.

(8) Cheng, L.; Liang, L.; Li, L. Nano-Ag colloids assisted tunneling mechanism for current conduction in front contact of crystalline Si solar cells. *2009 34th IEEE. PVSC* **2009**, 002345–002348

(9) Carroll, A. Screen printed metal contacts to Si solar cells – formation and synergistic improvements. *2013 IEEE 39th PVSC* **2013**, 3435–3440.

(10) Liang, L.; Li, Z.; Cheng, L.; Takeda, N.; Carroll, A. Microstructural characterization and current conduction mechanisms of front-side contact of n-type crystalline Si solar cells with Ag/Al pastes. *J. Appl. Phy*s. **2015**, 117, 215102.

(11) Burrows, M.; Meisel, A.; Balakrishnan, D.; Tran, A.; Inns D.; Kim, E.; Carroll, A.; Mikeska, K. Front-side Ag contacts enabling superior recombination and fine-line performance. *2013 39th IEEE. PVSC* **2013**, 2171–2175.

(12) Li, Z.; Mikeska, K.; Liang, L.; Meisel, A.; Scardera, G.; Cheng, L.; VerNooy, P.; Lewittes, M.; Lu, M.; Gao, F.; Zhang, L.; Carroll, A.; Jiang, C. Microstructural characterization of front-side Ag contact of crystalline Si solar cells with lightly doped emitter. *2012 38th IEEE. PVSC* **2012**, 002196–002199.

(13) Li, Z.; Mikeska, R.; VerNooy, P.; Liang, L. Microstructural investigation of new thick-film paste flux for contacting silicon solar cells. *2011 37th IEEE. PVSC* **2011**, 003659–003662.

(14) Li, Z.; Liang, L.; Cheng, L. Electron microscopy study of front-side Ag contact in crystalline Si solar cells. *J. Appl. Phys*. **2009**, 105, 066102.

(15) Li, Z.; Liang, L.; Ionkin, A.; Fish, B.; Lewittes, M.; Cheng, L.; Mikeska, K. Microstructural comparison of silicon solar cells' front-side Ag contact and the evolution of current conduction mechanisms. *J. Appl. Phys*. **2011**, 110, 074304.

(16) Zhou, Y.; Yang, Y.; Huang, F.; Ren, J.; Yuan, S.; Chen, G. Characterization of new tellurite glasses and crystalline phases in the TeO_2-PbO-Bi_2O_3-B_2O_3 system. *J. Non-Cryst. Solids* **2014**, 386, 90–94.

(17) Cai, X.; Teng, Y.; Wu, L.; Chan, X. Characterization of TeO_2 based glass frits and morphology to their silver films. *J. Mater. Sci: Mater. El*. **2017**, 28, 18429–18436.

(18) Qin, J.; Zhang, W.; Bai, S.; Liu, Z. Effect of Pb-Te-O glasseson Agthick-film contactincrystallinesilicon solar cells. *Sol. Energy Mat. Sol. C* **2016**, 144, 256–263.

(19) Zheng, G.; Tai, Y.; Wang, H.; Bai, J. Effect of the Pb-Te-B-O system glass frits in the front contact paste on the conversion efficiency of crystalline silicon solar cells. *J. Mater. Sci: Mater. El.* **2014**, 25, 3779–3786.

(20) Emique, C.; Sara, O.; Dominik, R.; Joachim, G.; Radovan, K.; Daniel, R.; Gunnar, S. Impact of Si surface topography on the glass layer resulting from screen printed Ag-paste solar cell contacts. *2012, 38th IEEE. PVSC* **2012**, 000204–000208.

(21) Pi, X.; Cao, X.; Chen, J.; Zhang, L.; Fu, Z.; Wang, L.; Zhang, Q. Improved Ag-Si interface performance for Si solar cells using a novel Te-based glass and recrystallization process of Ag. *Rare Metals* **2014**, 1–6.

(22) Shizuharu, W.; Takayuki, K.; Takashi, O. Influence of tellurite glass on reaction between Si_3N_4 anti-reflection coating film and Ag paste for electrodes in Si solar cells. *J. Ceram. Soci. JPN* **2016**, 124, 218–222.

(23) VerNooy, P.; Torardi, C.; Li, Z.; Lewittes, M.; Getty, R.; Mikeska, K.; Ionkin, A.; Cheng, L.; Wu, A.; Laughlin, B.; Laudisio, G. High-efficiency lead-free silver pastes for crystalline silicon solar cells. *2012, 38th IEEE. PVSC* **2012**, 002271–002273.

(24) Eisele, S.; Roder, T.; Ametowobla, M.; Bilger, G.; Werner, J. H. 18.9% efficient silicon solar cell with laser doped emitter. *2009, 34th IEEE. PVSC* **2009**, 000883–000885.

(25) Sharma, L.; Batra, S. Characterization and thermoanalytical investigations of silver tellurite. *J. Therm. Anal.* **1989**, 35, 2199–2212.